

Growth of magnetron sputtered TiO₂ thin films studied by X-ray scattering

R. Kužel^{1*}, L. Nichtová¹, D. Heřman², J. Šícha², J. Musil²

¹Department of Condensed Matter Physics, Faculty of Mathematics and Physics, Charles University in Prague, Ke Karlovu 5, 121 16 Praha 2, Czech Republic;

²Department of Physics, Faculty of Applied Sciences, University of West Bohemia, P.O. Box 314, 306 14 Plzeň, Czech Republic;

*Contact author; e-mail: kuzel@karlov.mff.cuni.cz.

Keywords: titanium oxide, thin film growth, X-ray diffraction, thin films

Abstract. Two sets of nanocrystalline TiO₂ thin films magnetron deposited on glass and silicon substrates have been studied by X-ray scattering and measurements of contact angle of water drop on the film surface. Phase analysis and X-ray line broadening were studied by X-ray powder diffraction in parallel beam optics, the residual stresses were measured with the aid of the Eulerian cradle and surface roughness determined by X-ray reflectivity measurement. By both thickness dependence of XRD patterns and depth profiling measurements it was found that rutile growths on the substrate and it is transformed to anatase with increasing distance from the substrate.

Introduction

Titanium dioxide films are widely used because of their excellent properties as chemical stability, mechanical hardness and optical transmittance with high refractive index. The photocatalytic activity of TiO₂ [1-3] can result in the decomposition of organic compounds on the TiO₂ surface or the reduction of the contact angle between water and the TiO₂ surface under ultraviolet irradiation (excellent hydrophilicity) [see 4 for more references]. The films can be prepared by several techniques but the magnetron deposition is favourable from the point of view of mechanical durability required for practical applications. Depending on the deposition conditions, the films can be prepared as amorphous or nanocrystalline.

The amorphous TiO₂ films do not have good hydrophilicity. Therefore, crystalline form of the oxide is required. This can be obtained either by annealing of amorphous films [4] or by setting of deposition parameters in such a way that crystalline or nanocrystalline films are obtained immediately. It seems that the latter way gives better results and it is preferred. Studies of different sets of TiO₂ films are described in [5]. For crystalline films, X-ray scattering is of particular interest in structural studies of these films because the whole potential of the technique can be used (phase analysis, strain, crystallite size, texture, stresses, surface roughness etc.).

In the present work, the deposited nanocrystalline films with different thickness and films prepared at different oxygen pressure were studied by X-ray diffraction.

Experimental

A complex XRD study was performed on TiO_2 films sputtered by dual magnetron equipped with two Ti(99.5) targets of 50 mm in diameter and supplied by a dc-pulsed Advanced Energy Pinnacle Plus+ 5kW power supply unit operating in bipolar asymmetric mode at repetition frequency $f_r = 100\text{kHz}$ and duty cycle $\tau/T = 0.5$; here τ and T are the length of pulse and the period of pulses. Films were deposited on unheated microscope glass slides ($26 \times 26 \times 1\text{ mm}^3$) and silicon (100) substrates ($26 \times 26 \times 1\text{ mm}^3$) at substrate to target distance $d_{s-t} = 100\text{ mm}$, total working pressure $p_T = 0.9\text{ Pa}$, average pulse discharge current $I_{da1,2} = 3\text{ A}$ and average pulse power density $W_{da} \approx 55\text{ Wcm}^{-2}$. Maximum substrate surface temperature during the deposition was lower than $T_{surf} \leq 160\text{ }^\circ\text{C}$. Further details on dual magnetron system are given elsewhere [6].

Two sets of samples were studied. Nanocrystalline TiO_2 films with different thickness $h = 100, 220, 515, 935, 2000\text{ nm}$ were deposited on the glass and silicon substrates in the oxide mode of sputtering at oxygen partial pressure $p_{O_2} = 0.15\text{ Pa}$ and deposition rate $a_D = 9\text{ nm/min}$. The other samples with the thickness of $h \approx 1000\text{ nm}$ were deposited at different oxygen partial pressure $p_{O_2} = 0.05\text{ Pa}, 0.085\text{ Pa}$ and 0.15 Pa with deposition rates $a_D = 45\text{ nm/min}, 20\text{ nm/min}$ and 9 nm/min . Both sets of samples are currently also annealed in order to find stability of the nanostructure.

The measurements were performed mainly on Philips X'Pert MRD in parallel beam setup, 2θ scans with the angles of incidence $0.5\text{--}1.5^\circ$ with parallel plate collimator placed in the diffracted beam and the Goebel mirror inserted in the primary beam. For a few measurements also - XRD7 (FPM-Seifert) diffractometer was used. In these measurements, phase analysis and X-ray line profile analysis were mainly performed. The measurements of residual stresses were carried out by using a polycapillary and Eulerian cradle by the $\sin^2\psi$ method for several different peaks. In addition, X-ray reflectivity curves were measured for all the samples.

Results

Diffraction patterns of the nanocrystalline films with different thickness are clearly distinct. The patterns for thin films (thickness 100 and 220 nm) show dominating rutile phase with a small indication of anatase (figure 1).

For thicker films (above 500 nm) anatase phase is dominating (figure 2) and nearly no lines of rutile could be found for the film with the thickness of 2000 nm. Essentially, this is true for both glass and single crystalline silicon substrates. Therefore, it seems that rutile growths on the interface with the substrate and it is gradually replaced by anatase with increasing distance from the substrate. For confirmation of the hypothesis, the depth profiling was performed by 2θ scans at several very small angles of incidence γ starting above the angle of total reflection at 0.5° . For these angles of incidence, the effective penetration depth is very sensitive to the value of the angles and increases rapidly with them. Observed profiles for the sample 515 nm thick are shown in figure 3. Effective penetration depths are increasing from about 100 nm to 400 nm for the angles γ changing from 0.5 to 2.0° . It can clearly be seen that the rutile peak is nearly absent for the smallest γ and it is significantly increasing with higher penetration depth. This behavior was found for both thinner and thicker films and also for both substrates which confirms the above speculation about the growth of rutile on the

interface. However, we cannot conclude from the measurements yet, whether there is only pure rutile on the interface or some amount of anatase is also present there.

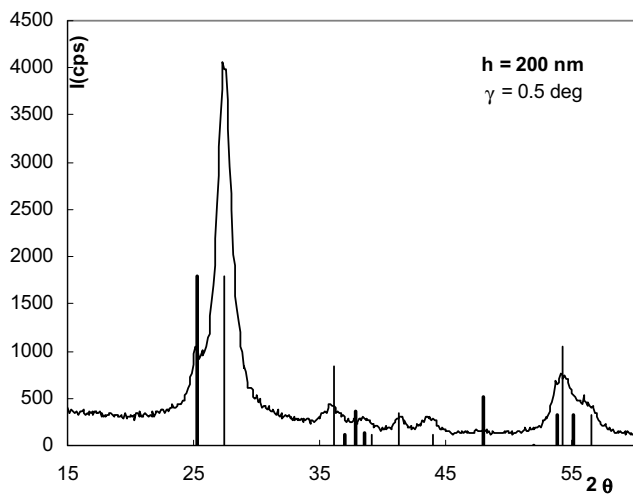


Figure 1. The first part of the diffraction pattern (2θ scan, angle of incidence 1.5°) for TiO_2 film 200 nm thick. The bars correspond to theoretical positions for diffraction peaks of anatase (thick) and rutile (thin).

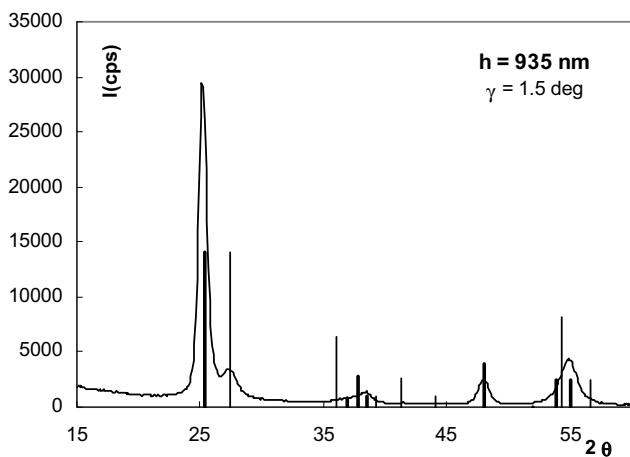


Figure 2. The first part of the diffraction pattern (2θ scan, angle of incidence 1.5°) for TiO_2 film 1000 nm thick. The bars correspond to theoretical positions of diffraction peaks of anatase (thick) and rutile (thin).

Line broadening has been estimated by the peak profile fitting and Williamson-Hall plot (i.e. the dependence of the integral breadth on the magnitude of the diffraction vector). Total powder pattern fitting has not been very successful yet in this case by any program. The Rietveld type programs usually did not include appropriate absorption and texture corrections for 2θ scans of thin films. We are still working on more correct evaluation of the full patterns of these nanocrystalline thin films. In general, the problem is complicated by possible simultaneous stresses and textures. Therefore in this case, the diffraction pattern has been divided into several segments and clusters of peaks fitted without structural constraints. However, because of very large broadening, this method is approximate and fitting must be made carefully and by fixing individual parameters during refinement (for example peak positions are approximately known and can be fixed at least for the first refinement cycles) and visual control of the decomposition. In this way, reasonable estimations can be made. The broadening is caused mainly by the crystallite size which is in nano scale and 6 - 7 nm for both rutile phase in thinner films and anatase in 500 and 935 nm thick films. The size of anatase crystallites was estimated to 10 nm for the thickest film (2000 nm).

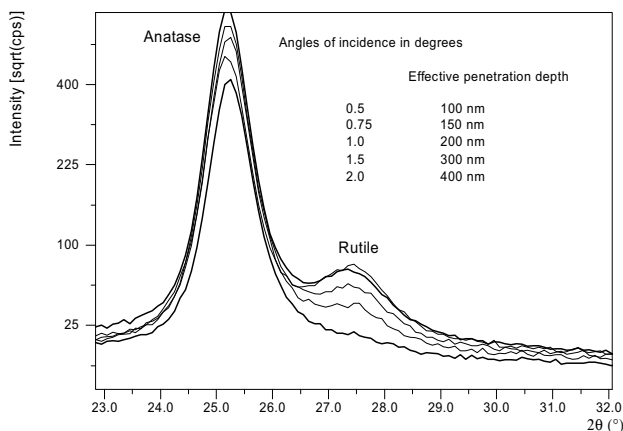


Figure 3. 101 peak of anatase and 110 peak of rutile scanned at several angles of incidence γ as indicated in the picture (0.5, 0.75, 1.0, 1.5, 2.0 °) for the film 515 nm thick. Effective penetration depths (shown in the right column) are increasing with the angles and monotonous corresponding increase of rutile peak can be seen. The bottom curve corresponds to $\gamma = 0.5^\circ$ (100 nm).

Measurement of the water droplet contact angle on the film surface after UV irradiation shown that the angle did not significantly drop from the initial value of about 80° even after long irradiation for two thinner samples (100, 220 nm) with dominating rutile phase. By contrast, it is reduced below 20° after 300 min UV irradiation for all the three thicker samples with dominating anatase phase. Reflectivity measurements (figure 4) indicate differences in surface roughness between thinnest films. As expected it is increased with increasing thickness. It seems that the different hydrophilicity is not simply related just to the surface roughness and it is more related to crystallinity and phase composition.

Stress and texture measurements with the aid of Eulerian cradle and ψ scans revealed that the texture is usually inclined and/or not of fibre type. This is closely related to the deposition process which is not axially symmetric for dual magnetron. As a consequence of this type of

texture, the $\sin^2\psi$ plots are of complicated and oscillating type and cannot be simply evaluated. However, general slope is rather small which also means small stresses.

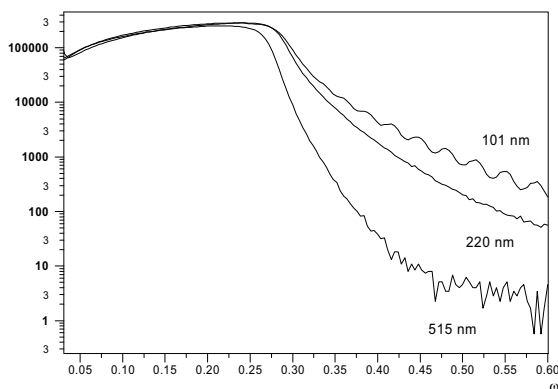


Figure 4. Reflectivity curves for the films 100, 220, 515 nm thick, respectively, from the top. Faster decrease of the reflectivity curves with increasing thickness indicates increasing surface roughness.

The diffraction patterns for the second set of samples (prepared with different partial oxygen pressure) are shown on figure 5. They are very different. For low pressure (0.05 Pa), amorphous films are obtained (figure 5a). They have poor hydrophilicity after UV irradiation. With medium pressures (0.0875 Pa, figure 5b) mixture of anatase and rutile was obtained. In this case, crystallite size of 20 and 6 nm was estimated for anatase and rutile respectively. Rutile has smaller crystallites which seems to be typical for a mixture of both phases. Microstrain of about 0.6 % was estimated for anatase. The higher pressure (0.15 Pa) leads to dominating anatase in the film (figure 5c). As expected, this particular film corresponds to the first set of samples and small indication of rutile peak may be related to the occurrence of the phase at the substrate interface. Crystallite size of 9 nm and microstrain of 0.3 % were estimated for the sample.

Both samples prepared at medium and higher oxygen pressure have excellent hydrophilicity after UV irradiation. The water droplet contact angle on the film decreased below 10° .

Conclusions

Nanocrystalline magnetron sputtered TiO_2 films were studied by XRD. It has been found that rutile growths on the interface with both Si and glass substrates. Then it is replaced by anatase with increasing distance from the substrate. This has been confirmed by studies of set of samples with different thickness as well as by glancing-angle XRD at very low angles of incidence and it could be caused by temperature gradient in the film during the deposition. The stresses in as-deposited nanocrystalline films were small (< 100 MPa) but complicated (triaxial, possible gradients). Texture is not always fibre and it may be inclined with respect to the surface. Current studies may lead to conclusions that for good hydrophilicity after UV irradiation the films should not be amorphous but preferably nanocrystalline.

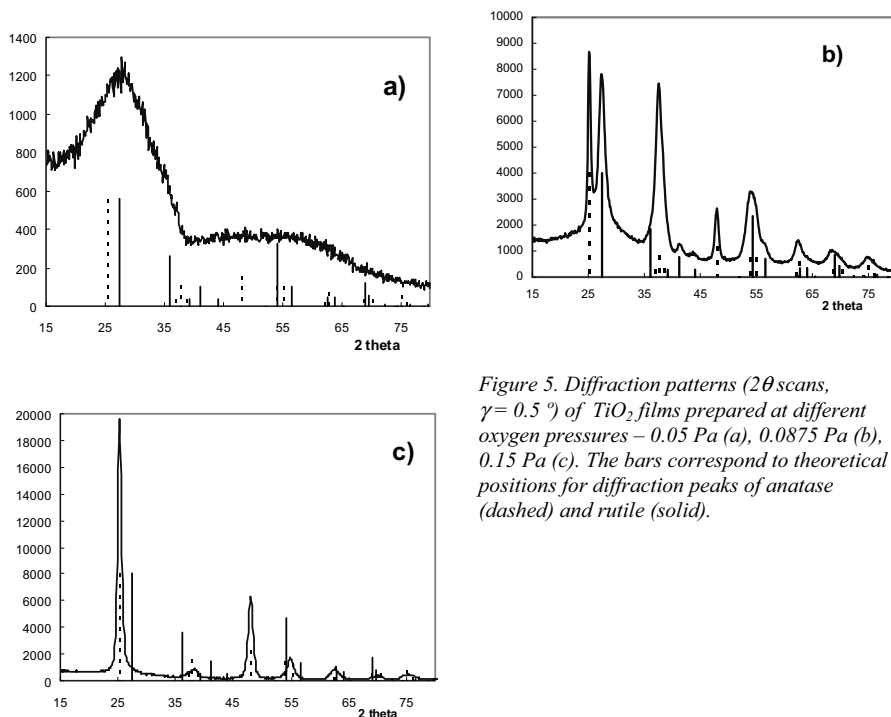


Figure 5. Diffraction patterns (2θ scans, $\gamma = 0.5^\circ$) of TiO_2 films prepared at different oxygen pressures – 0.05 Pa (a), 0.0875 Pa (b), 0.15 Pa (c). The bars correspond to theoretical positions for diffraction peaks of anatase (dashed) and rutile (solid).

References

1. Sopyan, N., Watanabe, M., Murasawa, S., Hashimoto, K & Fujishima, A., 1996, *J. Photochem. Photobiol.*, **A98**, 79.
2. Byun, I., Jin, Y., Kim, B., Lee, J.K. & Park, D., 2000, *J. Haz. Mat.*, **B73**, 199.
3. Negishi, J., Takeuchi, M. & Ibusuki, T., 1998, *J. Mater. Sci.*, **33**, 5789.
4. Kužel, R., Nichtová, L., Matěj, Z., Heřman, D., Šícha, J. & Musil, J., 2007, *Zeitschrift für Kristallographie (Supplement)*, this issue.
5. Musil, J., Heřman, D. & Šícha, J., 2006, *J. Vac. Sci. Technol.*, **A24** (3), 521-528.
6. Baroch, P., Musil, J., Vlcek, J., Nam, K.H. & Han, J.G., 2005, *Surf. Coat. Technol.*, **193**, 107.

Acknowledgements. The work is supported by the Grant Agency of the Czech Republic under number 106/06/0327 and also as a part of the research plans MSM 0021620834 and MSM 4977751302 financed by the Ministry of Education of the Czech Republic.